Aviation Electronics, Information Technology, Telecommunications, Electricals, and Controls (AVITEC)
Vol. 8, No. 1, February 2026, pp. 183-199, p-ISSN 2685-2381, e-ISSN 2715-2626
http://dx.doi.org/10.28989/avitec.v8i1.3686

Research Article

Voltage Drop and Power Loss Mitigation on SGN-14 via SGN-15 Feeder Design in Distribution System ULP Magelang

Haqrodji Prabu Yasya, Deria Pravitasari*, Agung Trihasto, Andriyatna Agung Kurniawan
Department of Electrical, Mechatronics, and Information Technology, Tidar University, Indonesia

Article Info

Article history:
Submitted December 5, 2025
Accepted January 21, 2026
Published February 20, 2026

Keywords:
Voltage drop;
power loss;
power distribution system;
optimization;
distribution network reconfiguration.

ABSTRACT

Feeder SGN-14 of PT PLN (Persero) ULP Magelang operates under overload conditions, significantly degrading voltage quality and increasing technical losses. PLN (Perusahaan Listrik Negara) is Indonesia's State Electricity Company, while ULP (Unit Layanan Pelanggan) refers to a customer service unit. This study designs Feeder SGN-15 as a 20 kV load-splitting feeder supplied from Sanggrahan Substation and terminating near KH. Maksum Street (Tempuran). The feeder is 20.7 km long and routed close to the load centre to reduce line losses. Network performance is assessed using ETAP load-flow simulations and independent GNU Octave calculations of voltage profile, current, and power/energy losses, referenced to SPLN T6.001:2013 with a 10% voltage-drop limit. The proposed feeder uses 8,152 m of insulated MVTIC and 12,584 m of AAAC conductors, supported by 238 concrete poles, together with required switching devices, line accessories, and four CSP transformers. After reconfiguration, the maximum voltage drops on SGN-14 decreases from 12.82% to 6.5%, while SGN-15 operates at about 4.95%, ensuring all buses comply with SPLN T6.001:2013. Technical losses on SGN-14 fall from 388.711 to 112.337 (W/kWh), and SGN-15 contributes 81.130 (W/kWh), giving total post-reconfiguration losses of 195.467 (W/kWh). The reduction in energy-loss cost yields an estimated saving of Rp228.82 million per month, lowering losses from Rp460.32 million/month to Rp231.44 million/month. Unlike studies that optimize only switch states or voltage-regulator placement, this work shows that adding a new 20 kV feeder can jointly improve voltages, reduce losses, and deliver tangible benefits for the distribution utility.

Corresponding Author:
Deria Pravitasari,
Department of Electrical Engineering, Mechatronics, and Information Technology, Tidar University, Indonesia
Email: *deria.pravitasari@untidar.ac.id

1. INTRODUCTION

Rapid load growth in urban distribution networks often pushes medium-voltage feeders beyond their thermal and voltage limits, leading to severe power losses and unacceptable voltage drops. International research has shown that metaheuristic algorithms such as binary particle swarm optimization [1] and grey wolf-optimized combinations of reconfiguration, distributed generation (DG) and capacitor placement [2] can effectively select switch states to reconfigure feeders and enhance voltage profiles. More recently, deep reinforcement-learning methods have been employed to sample feasible switch operations and learn optimal reconfiguration actions, outperforming traditional heuristics in loss reduction [3]. Emerging techniques such as undirected-graph isolation group detection combined with whale optimization offer additional improvements by efficiently identifying feasible radial topologies and eliminating infeasible islanding configurations [4].

The overload of 20 kV Feeder SGN-14 in the PT PLN (Persero) ULP Magelang distribution network exemplifies these challenges, PLN is (Perusahaan Listrik Negara) / State Electricity Company in Indonesia and ULP (Unit Layanan Pelanggan) / Customer Unit. While adjacent feeders retain spare capacity, SGN-14 suffers excessive line losses and under voltages at its remote ends. To remedy this imbalance, PLN is planning a new feeder, SGN-15, to off-load a portion of SGN-14's demand. Comparable studies demonstrate that linear optimization models for feeder reconfiguration and placement of voltage regulators can optimize network topology and improve voltage profiles [5], while particle swarm optimization combined with DG compensation

has achieved losses reductions exceeding 70 % in real networks [6]. Other works advocate distributed scheduling strategies based on blockchain-enabled alliance chains to optimally allocate source–load–storage resources [7], and highlight that careful placement of renewable and conventional DG units within a radial network can enhance voltage regulation and minimize losses [8]. These findings underpin the rationale for designing Feeder SGN-15 as a practical expansion to redistribute load and improve service quality in Magelang.

Maintaining voltage quality within ±5–10 % of nominal values is a fundamental requirement in medium-voltage distribution networks. Robust optimization frameworks have therefore been developed to maximize load supply under line and renewable-generation failures, using two-stage models that partition the network and dispatch flexible resources while respecting voltage constraints [9]. Economic dispatch models that incorporate network reconfiguration decisions into the scheduling of dispersed wind power demonstrate that such integration improves voltage regulation and lowers operating costs [10]. Reliability-driven dynamic reconfiguration strategies employing deep reinforcement learning further address uncertainty by selecting optimal switch actions that reduce power losses, voltage deviations and failure rates [11]. These studies highlight the need for feeder-planning solutions that balance technical performance with reliability and resilience.

Recent literature increasingly pursues integrated approaches to reconfiguration. Coordination of feeder reconfiguration with mobile energy storage fleets has been shown to reduce load shedding and accelerate restoration under forecast uncertainty [12]. Genetic-algorithm-based frameworks consider load margins and contingencies to derive resilient reconfiguration schemes that maintain service continuity during faults [13]. Comprehensive reviews classify existing techniques into heuristic, metaheuristic and machine-learning categories, emphasizing the growing adoption of data-driven and hybrid methods [14]. Dynamic reconfiguration algorithms that incorporate uncertainty modelling and co-evolutionary search efficiently adjust radial networks to stochastic variations in load and DG, reducing losses while enforcing voltage limits [15]. Together, these advances illustrate the breadth of optimization and control techniques applied to modify existing network topologies.

Although feeder reconfiguration is well-known to alleviate overloads and reduce losses in radial distribution networks [16][17], existing studies seldom articulate the specific gap addressed or combine both simulation and analytical tools in one framework. To our knowledge, no prior work has applied a dual ETAP-Octave approach to optimize an existing feeder (SGN-14) and design a new feeder (SGN-15) for simultaneous voltage-drop and loss mitigation. Therefore, this paper addresses that gap by formulating and solving a feeder-reconfiguration problem for the SGN system using both detailed ETAP power flow modeling and supporting Octave code for loss and drop calculations. The main objectives are to optimize feeder switching to minimize voltage drop, power loss, and energy loss while maintaining an acceptable voltage profile, and to compare these results against literature benchmarks. We explicitly demonstrate, for example, loss reductions comparable to those reported in recent studies (e.g. ~75% loss cut with smarter reconfiguration [16] and ~80% with DG integration [18]).

Nevertheless, most prior contributions focus on reconfiguring or compensating within the existing distribution framework. Recent proposals for dynamic topology reconfiguration aim to enhance photovoltaic (PV) hosting capacity, yet they remain limited to switching operations within current feeders [19]. Fault reconfiguration approaches employing improved discrete multimodal multi-objective particle swarm optimization address multimodal solution landscapes but still operate on existing feeders [20]. Fast reconfiguration methods using convolutional neural networks accelerate loss-reduction calculations for low-carbon distribution networks yet likewise avoid infrastructure expansion [21].

This research is conducted to resolve the overload problem on Feeder SGN-14 by planning a load transfer to a new feeder SGN-15 in the Magelang City area. The main goal is to analyze the network and reduce voltage drop and losses through simulation using ETAP software. ETAP is chosen for its proven effectiveness in various studies. According to SPLN T6.001:2013, the standard allowable voltage drop is 10% of nominal voltage, which is used as a benchmark. From the simulations, the values of voltage drop, power loss, energy loss, and cost impact are calculated for Feeder SGN-14 before and after load splitting.

2. RESEARCH METHODS

This research is a quantitative applied study in an electric power distribution system. All analysis steps utilize numerical data (currents, voltages, line lengths, conductor types, and transformer loads) which are calculated and simulated to observe changes in network performance before and after the technical measures. The aim is not only to capture the existing overloaded condition of Feeder SGN-14, but also to prove that adding/designing the new Feeder SGN-15 can reduce voltage drop and power loss back within the SPLN T6.001:2013 standard limit (±10%). In addition to simulations, analytical calculations are performed using GNU Octave (with electrical formulas) to compute these values and to verify the simulation results.

2.1 Collecting Data

The study uses secondary data from PLN's existing operations in 2024 until 2025. Data collection requires several pieces of information: peak load data on the SGN 14 feeder, as shown in Figure 1. Single Line

Diagram SGN 14 feeder, conductor impedance data for the SGN 14 feeder, line length data for the SGN 14 feeder, SGN 15 Feeder Design Data, PLN Construction Standard Data, and PLN Construction Standard Price Data. This data can be found in PT.PLN (Persero) ULP Magelang Kota, PT PLN (Persero) UP3 Magelang, and Electrical Substation SGN 14 become subject research.

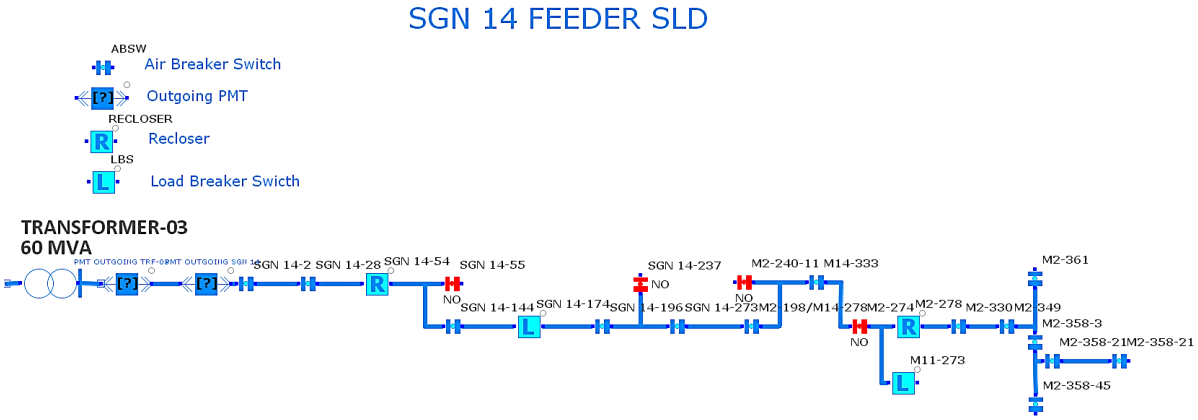

Figure 1. Single line diagram SGN 14 feeders

2.2 Technical Specification and Economic Research of SGN 15 Feeder Planning

Data planning of the SGN-15 feeder is carried out with two main focuses: technical and economic. On the technical side, it covers the selection and stringing of conductors or cables, types of poles, types of feeder accessories including protection devices, pole supports, pole extenders, service connections, network structures, transformers, operating schemes, and the feeder route along 20.7 km, as shown in Figure 2. SGN 15 feeder route so that SGN-15 can accommodate the transferred load from SGN-14 with voltage and reliability that meet the standards. On the economic side, the costs of materials, Laboure, profit, and taxes are calculated. Thus, this subsection emphasizes that the design of SGN-15 must be both technically and economically sound as a load-splitting solution for SGN-14 and all are listed in Table 1.

Table 1. Specification and Bill of Quantity (BOQ)

Install				Dismantle				BOQ
Category	**Item**	**Sum**	**Unit**	**Category**	**Item**	**Sum**	**Unit**	
Cable	AAAC 240, MVTIC 240	20.736	Meter	**Cable**	AAAC, MVTIC 70, AAAC 240	2.341	Meter	Rp4.497.139.229
Pole	Concrete Pole	238	Pole	**Pole**	Concrete Pole, Steel Pole	60	Pole	Rp1.599.003.099
Operation	ABSW, LBS, Transformer	8	Unit	**Operation**	ABSW, LBS, Transformer	8	Unit	Rp393.776.786
Feeder Accessories	Fuse Cut Out, Arrester, Grounding, Extender Pole, Strenghten Pole	838	Unit	**Feeder Accessories**	use Cut Out, Arrester, Grounding, Extender Pole	149	Unit	Rp465.070.583
Line Construction	Medium Voltage Twisted Insulated Cable Line Construction, Medium Voltage Line Construction, Low Voltage Line Construction	943	Unit	**Line Construction**	Medium Voltage Twisted Insulated Cable Line Construction, Medium Voltage Line Construction, Low Voltage Line Construction	360	Unit	Rp1.958.206.832

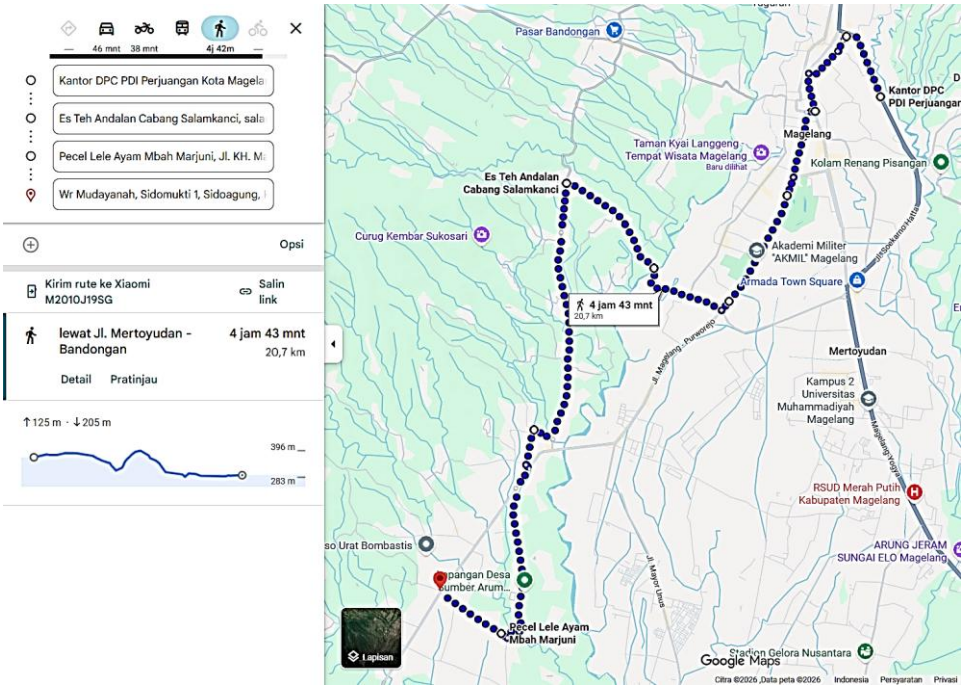

Figure 2. SGN 15 feeder route

2.3 SGN 14 and 15 Feeder Data Analyze

SGN-14 and SGN-15 Feeder Data Analyze outlines the network data that form the basis for the modelling and analysis in the results and discussion chapter. In Table 2, SGN 14 feeder condition part, the data of Feeder SGN-14 are first presented, including the arrangement of sections and pole numbers, location spans between key substations/landmarks, section lengths, the types of conductors used, and supporting information such as load connection points and operating configuration that will later be used as input for load-flow simulations. Subsequently, the data Table 3, SGN 15 feeder palning are described in a similar manner, covering pole numbering, location segments from GI Sanggrahan to the end of the feeder, distance per section, and the types of conductors applied (such as MVTIC, AAAC, and SUTM) as part of the new feeder design. These network data are then represented in a Single Line Diagram generated using ETAP software, enabling the reader to clearly understand the topology and interconnection between buses on Feeder SGN-14 and SGN-15 before voltage-drop, load-flow, and loss analyses are carried out in the subsequent results and analysis chapter.

Table 2. SGN 14 feeder condition

Measurement Point			Average Current Measurement (A)	Breaker
Pole	Distance Per Section (km)	Conductor	RST	
M14-2	0,05	AAAC	255,3	PRIMARYABSW
M14-28	1,3	AAAC	251,3	ABSW
M14-54	1,3	AAAC	247,6	RECLOSER
M14-144	4,5	AAAC	243,6	ABSW
M14-174	1,5	AAAC	232,3	LBS
M14-196	1,1	AAAC	228	ABSW
M14-273	3,85	AAAC	222,3	ABSW
M2-198/M14-287A	0,7	AAAC	216,3	ABSW
M14-333	2,4	AAAC	207,6	ABSW
M2-274	4,95	AAAC	118,5	ABSW
M2-278	4,4	AAAC	100,75	RECLOSER
M2-330	3,05	AAAC	70	ABSW
M2-349	1,05	AAAC	56,6	LBS
M2-358-3	0,6	AAAC	38,75	ABSW
M2-358-21-1	0,95	AAAC	18,02	ABSW
M2-358-21-36-20	2,75	AAAC	7,23	ABSW
M2-361	2,9	AAAC	22,51	ABSW

Table 3. SGN 15 feeder planning

Pole	Location	Distance Per Section (km)	Conductor
PMT SGN 15	GI SANGGRAHAN	0.005	MVTIC
M15-95	GI - CPM	2.688	MVTIC
M2-135-B	CPM - PAKELAN	4.118	AAAC
M2-135X-3	PAKELAN - KEDUNGINGAS	1.064	MVTIC
M2-135X-42-76	KEDUNGINGAS - JOGOMULYO	6.879	SUTM
M2-215-1A-94	JOGOMULYO - SUMBERARUM	4.281	MVTIC
M2-253-1	JL KY. MAKSUM TEMPURAN	1.390	AAAC

2.4 Octave Calculation of Drop Voltage and Power Losses

The analytical calculation procedure using GNU Octave that complements the ETAP load-flow simulations in this study. In this part, the structure of the input data will be outlined first, including section lengths of the feeders, conductor parameters (resistance and reactance), load currents, operating time, and source/receiving-end voltages taken from the SGN-14 and SGN-15 feeder data. The subsection then explains how the basic equations for line impedance, voltage drop, percentage voltage deviation, active power loss, and energy loss are implemented in Octave—both in the form of computational scripts and a graphical user interface (GUI). The calculation flow (from data entry, processing, to result display) and the definition of output variables such as receiving-end voltage, ΔV, % voltage drop, power loss, energy loss, as well as the error and accuracy indices used to compare Octave results with ETAP simulations, are also described. In this way, Subsection 2.4 establishes the manual-calculation framework that will later be used in the results and analysis chapter to validate the simulation outcomes and to evaluate the consistency of voltage-drop and power-loss assessments on the SGN-14 and SGN-15 feeders.

2.4.1 Drop Voltage Calculation

Drop voltage like in Equation (1) and (2) is defined as the difference between the sending-end (source) voltage and the receiving-end (load) voltage in an electrical power system. This phenomenon naturally occurs due to the presence of resistance and impedance in the conductors that carry current along the distribution network. If the voltage drop exceeds the allowable limit, it can degrade power quality, cause lamps and motors to operate below their rated performance, and in more severe cases increase the risk of damage to customer equipment. Therefore, calculating the voltage drop along each section of the feeder is essential to ensure that the supplied voltage remains within acceptable service limits. In this study, the evaluation of voltage drop refers to SPLN T6.001:2013, which specifies that the maximum permissible voltage drop on low-voltage networks is 10% of the nominal voltage; this threshold is used as a benchmark to assess whether the designed and reconfigured feeders meet the required technical standards.

$$\Delta V = V_s - V_r \quad (1)$$

$$\%\, Voltage\ Drop = \left(\frac{V_s - V_r}{V_s}\right) x\ 100\% \quad (2)$$

with: ΔV : drop voltage (volt)
V_s : sent voltage (volt)
V_r : receive voltage (volt)
% Voltage Drop : percentage drop voltage (%)

Mathematically, the percentage voltage drop is evaluated using an expression that directly measures the difference between the sending-end voltage (V_s) and the receiving-end voltage (V_r) like in the equation (3), thereby indicating how much voltage is lost along the line. By dividing this difference by Vs and multiplying it by 100%, the result is normalized into a percentage, which provides a more intuitive indication of how significant the voltage reduction is relative to the initial voltage and allows a consistent comparison of performance across different feeders.

In the context of this study, the use of this formula is appropriate because the feeder can be modelled as a short transmission line, with a length of less than 50 miles (approximately 80 km). For determining the receiving-end voltage in volts in a three-phase distribution system, the calculation is then carried out using the following equation:

$$V_r = \sqrt{3}\ x\ I\ x\ L\ (R\ cos\ \theta + X\ sin\ \theta) \quad (3)$$

with: V_r : receive voltage (volt)
I : current (ampere)
L : conductor length (kilometer)
R : resistance conductor (ohm/km)
Θ : power factor
X : reactance conductor (ohm/km)

2.4.2 Power Loss Calculation

Power losses in Equation (4) are defined as the portion of electrical energy that is dissipated during transmission from the source to the load due to the resistance of the conductors. In general, these losses are categorized into two types. Technical losses are associated with the physical characteristics of system components, such as conductors, transformers, and other equipment, and are an inherent consequence of current flow. Non-technical losses, on the other hand, arise from factors such as improper installation, electricity theft, or inaccurate meter readings, which do not originate from the physical properties of the network itself. In distribution network studies, the main focus is typically on technical losses, as these can be quantified and reduced through proper design, conductor selection, and network reconfiguration.

$$\Delta P = 3 \; x \; I2 \; x \; R \; x \; L \tag{4}$$

with: ΔP : power losses (watt)
I : current (ampere)
R : resistance (ohm/km)
L : conductor length (kilometer)

Based on the calculated power losses, the corresponding energy losses over a given time interval can also be determined. In principle, energy loss represents the accumulated effect of power loss over the operating period, so that a feeder with a constant power loss but a longer operating time will produce a larger energy loss. This quantity is important because it can be directly converted into a monetary value using the applicable electricity tariff, thereby providing an indication of the economic impact of losses on the distribution system. In this study, the energy loss over a specified observation period is obtained from the power loss using the Equation (5).

$$E = P \; x \; t \tag{5}$$

with: E : energy losses (kilowatt per hour)
P : power losses (watt)
t : time (hour)

2.4.3 ETAP and Octave Accuracy

ETAP is software used to analyse power systems in a list-based environment, both offline for simulation and online for data acquisition. It supports various studies such as load flow, short-circuit, motor starting, arc-flash, power system harmonics, transient stability analysis, and protective device coordination, with help features that guide users in operating the program. One of its key components is the Single Line Diagram, a graphical tool for drawing and editing network diagrams; through this editor, users can refine, modify, and connect elements, adjust their size and orientation, hide symbols, and set protection parameters according to the needs of the analysis. Because the results are produced by a software tool, we must therefore perform accuracy testing using manual calculations or by comparing them with other software the formulas are explain in Equation (6) and (7). Figure 3 shown display GUI system in Octave is the appearance of the program.

$$\frac{|Result_{ETAP} - Result_{Octave}|}{Result_{ETAP}} \; x \; 100 \; \% \; = \; Error \; percentage \; \% \tag{6}$$

$$100 \; \% \; - \; Error \; percentage \; = \; ETAP \; Accuracy \; \% \tag{7}$$

with: $Result_{ETAP}$: simulation result
$Result_{Octave}$: calculation result

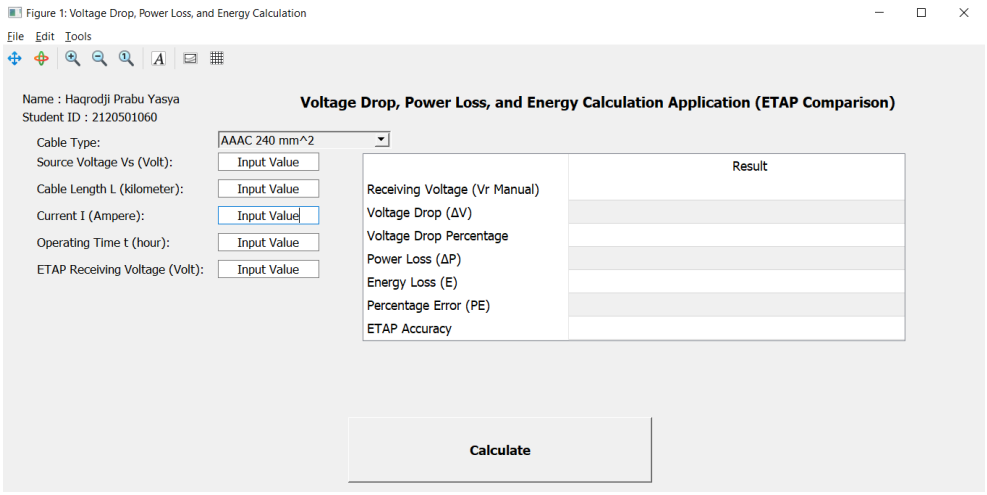

Figure 3. Display GUI system in Octave

2.5 ETAP Simulation of Drop Voltage and Power Losses

Numerical analysis performed using ETAP as a counterpart to the manual calculations in GNU Octave. In this part, the modelling procedure for the SGN-14 and SGN-15 feeders will be outlined, starting from the construction of the single line diagram, input of feeder section data (lengths, conductor types and impedances, transformer and load data), and the definition of operating scenarios before and after load redistribution. The subsection will explain the load-flow settings used in ETAP—such as base voltage, power flow method, loading conditions, and convergence criteria and how bus voltages, line currents, active power losses, and energy losses are obtained from the simulation outputs like in the figure below Figure 4. ETAP single line diagram display. It will also describe how specific result views (voltage profile, colored bus indicators, and loss reports) are extracted for each section along the feeders. Finally, this subsection clarifies that the ETAP simulation results will be used in the results and analysis chapter as the primary reference for evaluating voltage drop and power losses on SGN-14 and SGN-15, as well as for comparison and validation against the Octave-based analytical calculations.

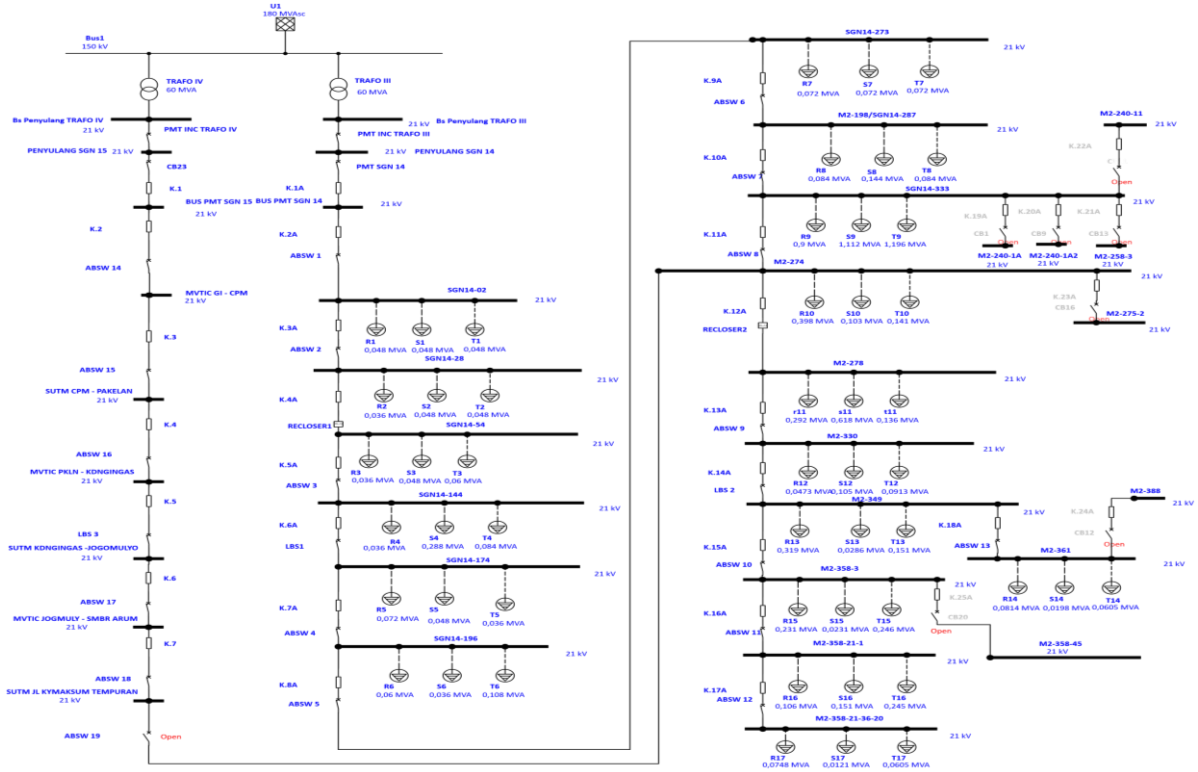

Figure 4. ETAP single line diagram display

2.6 Determination Reconfiguration Point

procedure used to select the optimal reconfiguration point between Feeder SGN-14 and the newly planned Feeder SGN-15. In this part, the criteria for choosing the reconfiguration point are first outlined, including feeder loading, voltage profile, location of major load concentrations, line losses, operational constraints, and field conditions such as existing switchgear and accessibility. The subsection then describes how several candidate points along SGN-14 are identified as potential splitting or tie locations, and how each candidate is evaluated through load-flow simulations in ETAP and supporting calculations in GNU Octave to assess its impact on voltage drop, current loading, and power losses under normal operating conditions. It also states that network constraints such as maintaining radial operation, ensuring proper protection coordination, and complying with utility planning standards are taken into account when comparing scenarios. Finally, this subsection clarifies that the selected reconfiguration point obtained from this procedure will serve as the basis for the detailed design and analysis of the SGN-15 feeder configuration presented in the subsequent chapters.

2.7 Analysis of Energy Loss Reduction

Approach used to quantify how far the proposed reconfiguration and the addition of Feeder SGN-15 can reduce energy losses in the distribution system. In this part, the methodology for comparing losses before and after reconfiguration on SGN-14 and SGN-15 will be outlined, starting from the extraction of line-by-line active power losses from ETAP load-flow simulations and the corresponding analytical results from GNU Octave. The subsection explains that energy losses over the assumed operating hours will be evaluated per section and for the total feeder, so that the overall impact of load transfer from SGN-14 to SGN-15 can be clearly

seen. It also states that percentage loss reduction will be calculated to show the improvement achieved by the new configuration, and that the reduction in energy losses will be further interpreted in terms of potential economic savings using the applicable electricity tariff. Thus, this subsection establishes the framework for assessing how effective the SGN-15 feeder design is in decreasing technical losses and improving the efficiency of the PT PLN (Persero) ULP Magelang distribution network.

2.8 Standardization

Focuses specifically on the Indonesian utility standard SPLN T6.001:2013 as the main technical reference for assessing the performance of the SGN-14 and SGN-15 feeders in this study. In this part, the key provisions of SPLN T6.001:2013 related to medium-voltage distribution will be outlined, with emphasis on the permissible voltage deviation limits along 20 kV feeders (10% of nominal) and their implications for service quality at customer connection points. The subsection will explain how these limits are used as benchmark criteria to judge whether the simulated bus voltages on SGN-14 and SGN-15 both before and after load redistribution are still within acceptable ranges, and how any sections that exceed the tolerance are identified as problem areas requiring mitigation. It will also clarify that Table 4. SPLN T6.001:2013 is adopted as the primary standard for evaluating the feasibility of the SGN-15 feeder design, ensuring that all technical analyses of voltage drop, power loss, and load transfer in the subsequent chapters are interpreted with respect to nationally recognized distribution-system performance requirements.

Table 4. SPLN T6.001.2013

Highest voltage for equipment (kV)	Nominal system voltage (kV)	Utilization
7.2[1)]	6[1)]	Generation
12[2)]	11[2)]	Generation
24	20	Distribution & Generation

* Three-phase, three-wire systems unless otherwise stated.
The values shown are phase-to-phase voltages.
[1)] This value is not used for public distribution systems.
[2)] No longer developed.
[3)] For four-wire three-phase systems.
The difference between the highest and lowest voltages shall not be greater than ±10% of the nominal system voltage.

3. RESULTS AND DISCUSSION

3.1 Analysis of Feeder SGN-15 Technical Specifications and Cost-Effectiveness

The design of Feeder SGN-15 is a strategic step to transfer a portion of the load from the overloaded Feeder SGN-14, thereby reducing the voltage drop and losses in PT PLN (Persero) ULP Magelang City's distribution network. The new feeder route is planned from the Sanggrahan Substation (source) in the northern Magelang corridor, passing through major activity centers (Rindam area, Armada Town Square, Mertoyudan) and extending southwest to its endpoint at KH. Maksum street Tempuran, with a total length of about 20.7 km. This route is chosen because it is close to load centers, faces minimal construction obstacles, and complies with SPLN standards on distance between poles, pole placement, and network configuration. The technical specifications are based on existing conditions and PLN standards, including selecting the conductor type/size, pole type, protection devices, and sectionalizing points, with an emphasis on ease of operation and maintenance. Structurally, the construction work is divided into six main sections: (1) installation of insulated twisted MV cable (SKUTM) from GI to CPM, (2) installation of MV overhead line (SUTM) from CPM to Pakelan (double-circuit with feeders SGN-02 & SGN-11), (3) reconductoring with MVTIC cable from Bayanan to Kedungingas, (4) installation of SUTM from Kedungingas to Jogomulyo (double-circuit with SGN-12 & SGN-15), (5) installation of SKUTM from Jogomulyo to Sumberarum, and (6) reconductoring the SUTM 70 mm² line to 240 mm² along KH. Maksum street Tempuran. This segmentation facilitates performance analysis for each portion in the results and discussion.

Technical specification for the feeder project is structured into five main categories that cover both installation of the new network and dismantling of the existing one. In the cable category, about 20.736 km of new AAAC 240 and MVTIC 240 are installed while 2.341 km of existing AAAC, MVTIC 70, and AAAC 240 are removed, making conductors the largest single cost component. For poles, 238 new concrete poles are erected and 60 concrete and steel poles are dismantled to match the new route layout. The operation category includes eight units of switching and protection equipment (ABSW, LBS, and transformers) that are installed and eight similar units dismantled or relocated, which, although few in number, contribute a notable share of the cost due to their technical specifications. Feeder accessories comprise 838 installed units and 149 dismantled units, covering fuse cut-outs, surge arresters, grounding sets, pole extenders, and strengthening hardware that ensure mechanical integrity and electrical protection of the line. Finally, line construction consists of 943 new

construction and 360 dismantled construction units, including medium-voltage twisted insulated cable structures, conventional medium-voltage overhead line structures, and low-voltage structures; after conductors, this category together with poles forms the next largest cost portion in the BOQ, while operating equipment and accessories account for smaller but still essential investments needed to complete the new feeder and its reconfiguration.

As summarized in the cost section of Table 1, the bill of quantity for the SGN-15 feeder results in a subtotal for goods and services of Rp. 8,893,715,077. Key cost drivers in the budget are the cables and conductors, which account for the largest portion of the cost. The next highest expenses come from the poles (particularly concrete poles installation) and the medium-voltage network structures (JTM constructions). These categories involve significant material and labor investment. Other categories such as accessories, primary structures, operational units, and transformers constitute smaller fractions of the budget in comparison. On top of this the detail of total amount is explained in Table 5. Bill of Quantity, a 5% contractor's profit of Rp444,685,754 is applied, and an 11% tax adds a further Rp978,308,658. Consequently, the total investment cost for constructing the new SGN-15 feeder and carrying out the associated dismantling works is Rp10,316,709,489.

Table 5. Bill of Quantity

Bill of Quantity	Cost (IDR)
Total Goods and Services	8,893,715,077
Profit 5%	444,685,754
Tax 11%	978,308,658
Final Total	10,316,709,489

3.2 Feeder SGN-14 and SGN-15 Data (Existing Conditions)

Table 3 provides detailed data for Feeder SGN-14 in Sanggrahan Substation under existing conditions (before any reconfiguration). It lists the section-by-section measurements along SGN-14 from the substation to the end of the feeder. The table includes each section's pole number/measurement point, length, the peak load current in average phase (R, S, T), and the type of switching device at that point. As shown, the highest current near the source is about 255.3 A, using AAAC conductor with impedance 0.1344 + j0.3158 Ω/km. Measure of the current doing in the night. The total line distance is ~37.35 km for SGN-14.

The data for the SGN-15 feeder is presented in Table 4. At this stage, the load data has not yet been filled in because the feeder has not been reconfigured. The reconfiguration process involves combining two different conductors in each section—namely, AAAC with an impedance of 0.1344 + j0.3158 ohm/km and MVTIC with an impedance of 0.125 + j0.31 ohm/km—resulting in a total conductor length of 20.7 kilometers.

3.3 GNU Octave Calculation

Figure 5 shows a custom GNU Octave application developed to calculate voltage drop, power loss, and energy loss with a GUI interface. The left side allows input of technical data (source voltage, line length, current, operating time, and the *V_r* from ETAP for comparison), while the right side displays the automatic output: calculated receiving-end voltage, ΔV, % voltage drop, power loss, energy loss, as well as error and accuracy relative to ETAP. Upon clicking "Calculate," the application instantly provides results, enabling quick analysis without repetitive manual computation by applying equations (1) through (7) in the Octave GUI implementation. The following constant values are used in the calculations:

√3 = 1.73
R MVTIC = 0.125 Ω/km
R AAAC = 0.1344 Ω/km
X MVTIC = 0.31 Ω/km
X AAAC = 0.3158 Ω/km
θ (power factor angle) = 0.85 *(power factor ≈ 0.85)*
V PMT14 = 20,899 V (sending voltage of SGN-14 before switching)

Using this tool, Table 6 summarizes the Octave calculation results for voltage profile, voltage drop, and losses along Feeder SGN-14 *before* reconfiguration. Starting from the source (PMT SGN-14) with a high current (~254.8 A) and send voltage ~20.899 kV, each additional line segment causes a notable voltage drop and power loss. The current decreases gradually from about 250 A to 240 A by around point M14-333 (after more than 15 km of line), meaning the upstream segments still carry high current over long distances. Certain heavy-loaded spans—such as around pole M14-144 (ΔV ≈ 607.45 V or 3.049%), M14-273 (ΔV ≈ 473.36 V or 2.476%), and M14-333 (ΔV ≈ 275.21 V or 1.467%)—are the major contributors to the voltage reduction, due to the combination of still-high currents (>200 A) and long distance by those points. The cumulative drop across the entire feeder reaches about 2,874.21 V, which is 14.93% of the source voltage, exceeding the SPLN T6.001:2013 limit of ±10%. In other words, the feeder end is at a very low voltage level (~18 kV) and would be extremely sensitive to any further load increase. Correspondingly, the power losses escalate, totaling about 397,076 W (397 kW) for the feeder.

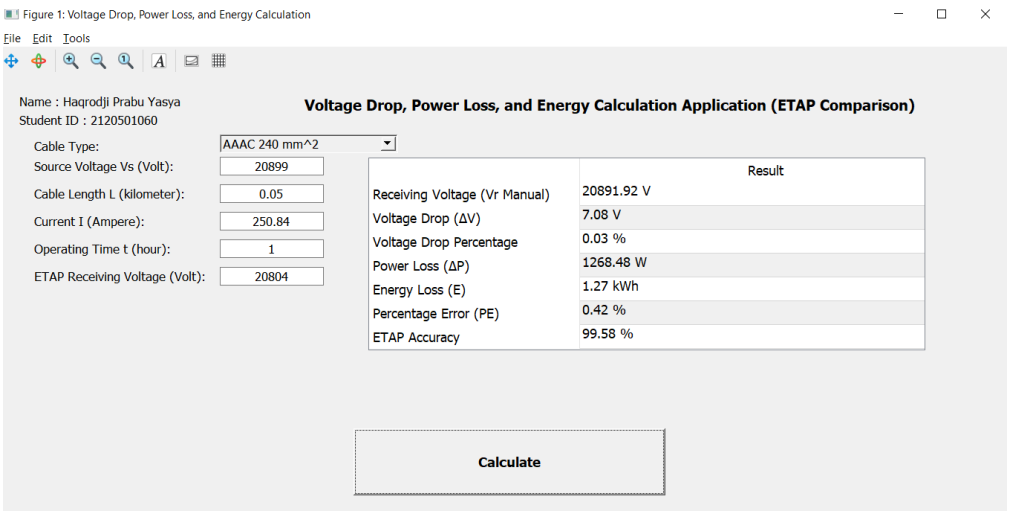

Figure 5. GNU Octave-based voltage drops and loss calculation tool (GUI) result

Table 6. Feeder SGN-14 Voltage Profile and Losses (Octave Calculation, Pre-Reconfiguration)

Pole Number	Distance Persection (km)	Load (A)	Manual Calculate Before Reconfiguration				
			Vr	Drop Voltage	Drop Voltage (%)	Power Loss (W)	Energi Loss (kwh)
PMT SGN 14	0.005	254.8	20.899	0.72	0	130	0,130
M14-2	0.05	250.8	20891	7.08	0.033890	1.268	1.268
M14-28	1.3	246.8	20709	181.11	0.874547	31.937	31.937
M14-54	1.3	243.1	20530	178.42	0.869070	30.994	30.994
M14-144	4.5	239.1	19922	607.45	3.049142	103.787	103.787
M14-174	1.5	227.8	19729	192.89	0.977692	31.397	31.39681
M14-196	1.1	223.5	19590	138.77	0.708363	22.156	22.156
M14-273	3.85	217.8	19116	473.36	2.476250	73.664	73.66421
M2-198/M14-287A	0.7	211.8	19032	83.69	0.439733	12.666	12.66585
M14-333	2.4	203.1	18756	275.21	1.467317	39.943	39.943
M2-274	4.95	114.0	18437	318.61	1.728065	25.956	25.956
M2-278	4.4	96.24	18198	238.99	1.313276	16.430	16.43
M2-330	3.05	65.52	18085	112.79	0.623659	5.279	5.2792
M2-349	1.05	52.1	18054	30.88	0.171041	1.149	1.14917
M2-358-3	0.6	34.26	18042	11.6	0.064294	283.95	0.28395
M2-358-21-1	0.95	18.02	18032	9.66	0.053571	124	0.124
M2-358-21-36-20	2.75	4.093	18025	6.35	0.035229	18.58	0.01858
M2-361	2.9	4.49	18047	7.35	0.040728	23.57	0.02357
	TOTAL			2874.21	14.925868	397.076	397.07634

3.4 Reconfiguration SGN 14 dan SGN 15 Feeder

3.4.1 SGN 14 Feeder

Figure 6 illustrates the voltage profile along Feeder SGN-14 as a function of distance before and after the network reconfiguration. with results from both ETAP and GNU Octave. Before reconfiguration. the feeder's voltage drops sharply as the distance increases – starting near 100% at the substation and falling to around 85–87% at the far end (approximately 37 km). This corresponds to a voltage drop on the order of 12.8–14.9%. which exceeded the allowable 10% limit defined by the SPLN T6.001:2013 standard. The steep decline is due to heavy loads being supplied over a long distance on SGN-14. causing large cumulative voltage drops in certain segments (e.g. spans with >200 A load saw drops of 2–3% each). After reconfiguration. the voltage profile improves markedly. The orange and yellow plots (ETAP and Octave post-reconfiguration) show that the feeder voltage now stays above 93% even at the new furthest load point. corresponding to only about a 6.5% drop from the source. In other words. SGN-14's end-voltage is brought back within standards. resolving the previous undervoltage issue. Both ETAP and Octave calculations align closely on these profiles. indicating that the simulation model is accurate – the Octave-computed voltages virtually overlap the ETAP results in Fig. 6.. which validates the reconfiguration's effect on voltage quality. Importantly. the post-reconfiguration profile complies with SPLN T6.001:2013's ±10% voltage deviation limit. This confirms that splitting the load with the new feeder has successfully stabilized SGN-14's voltage within acceptable range.

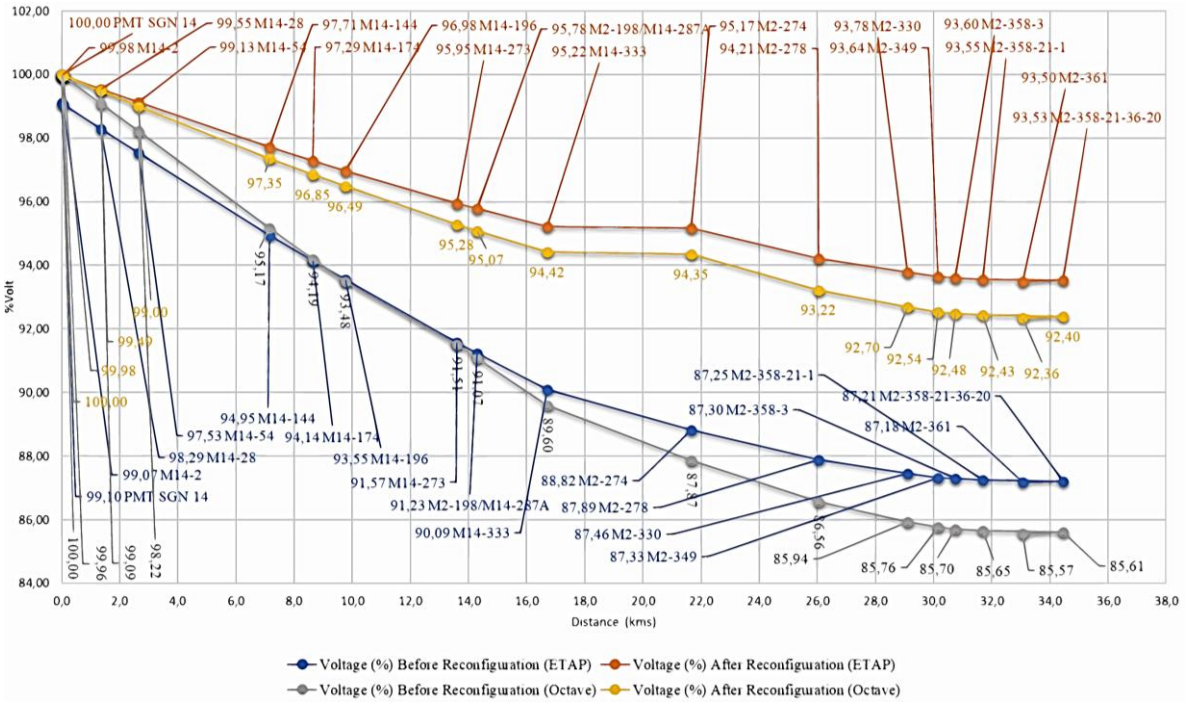

Figure 6. Voltage drop SGN 14 feeder before and after reconfiguration

Figure 7 presents a bar chart comparing the active power losses at each section of SGN-14 before vs. after reconfiguration. as obtained from ETAP and Octave. The blue/gray bars (pre-reconfiguration losses per node from ETAP/Octave) are significantly taller across most sections than the corresponding orange/yellow bars (post-reconfiguration losses). This indicates a substantial reduction in line losses after the network was reconfigured. Originally. the total power dissipated on SGN-14 was approximately 388.7 kW (sum of losses along the feeder). The highest losses occurred in the heavily loaded later segments of the feeder – for example. near the 15–25 km points. individual segment losses reached tens of kW. compounding to the high total. After reconfiguration. the loss at every segment drops dramatically because a significant portion of the load (and hence current) was transferred to the new feeder SGN-15. The new total losses on SGN-14 sum to only about 112.3 kW (a 71% decrease on that feeder). Visually. Figure 7 shows the after-reconfiguration bars at each node are much shorter – many previously high-loss sections now dissipate only a few kilowatts. Both the ETAP simulation and Octave manual calculation agree on the magnitude of these losses. as their bars nearly coincide. This close agreement (generally within a few percent difference) not only highlights the accuracy of the simulation but also reinforces that the reconfiguration yielded a pronounced reduction in resistive losses along SGN-14.

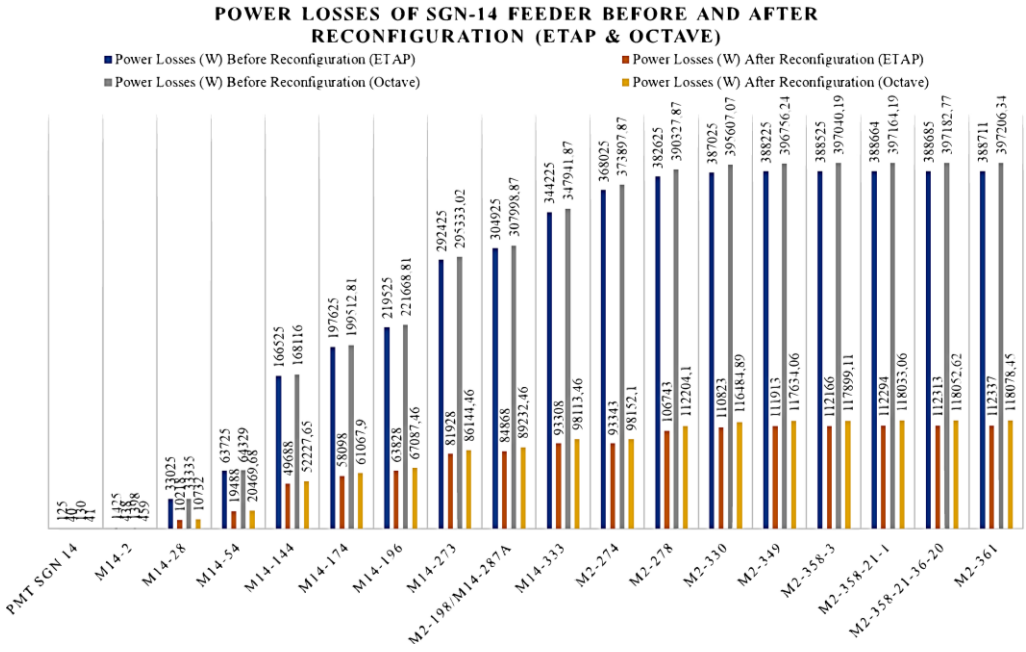

Figure 7. Graph power losses SGN 14 feeders before and after reconfiguration

The energy losses for SGN-14 before and after reconfiguration are compared in Figure 8. with each bar representing the energy lost (in kWh) at a given section over the analysis period. The overall pattern mirrors the power loss results. since energy loss is essentially the time-integrated power loss. Prior to reconfiguration. SGN-14's cumulative energy loss was about 388.7 kWh (assuming a one-hour period. equivalent numerically to the ~388.7 kW of power loss). These losses were concentrated toward the feeder's end. compounding due to prolonged high current flow over long distances. After the feeder reconfiguration. the energy loss per section dropped in tandem with the power losses – the orange and yellow bars in Fig. 8. (ETAP and Octave post-reconfig) are uniformly much shorter than the blue/gray bars (pre-reconfig). The total energy lost on SGN-14 is reduced to roughly 112.3 kWh. a savings of about 276 kWh compared to before (roughly a 71% reduction). This dramatic decrease reflects how much energy was being wasted as heat in the overextended original network. Now. with the load split. the distribution is more efficient. Notably. the ETAP and Octave results for energy loss are nearly identical at each point. confirming that the simulation's power-loss reduction translates directly into proportional energy savings. The post-reconfiguration energy losses along SGN-14 are not only lower in absolute terms. but they also indicate a more uniform and manageable loss profile consistent with a healthier feeder operation. This improvement is in line with expectations from literature on network reconfiguration and feeder offloading. which report significant loss reductions and improved efficiency when an overloaded feeder is relieved by a new feeder.

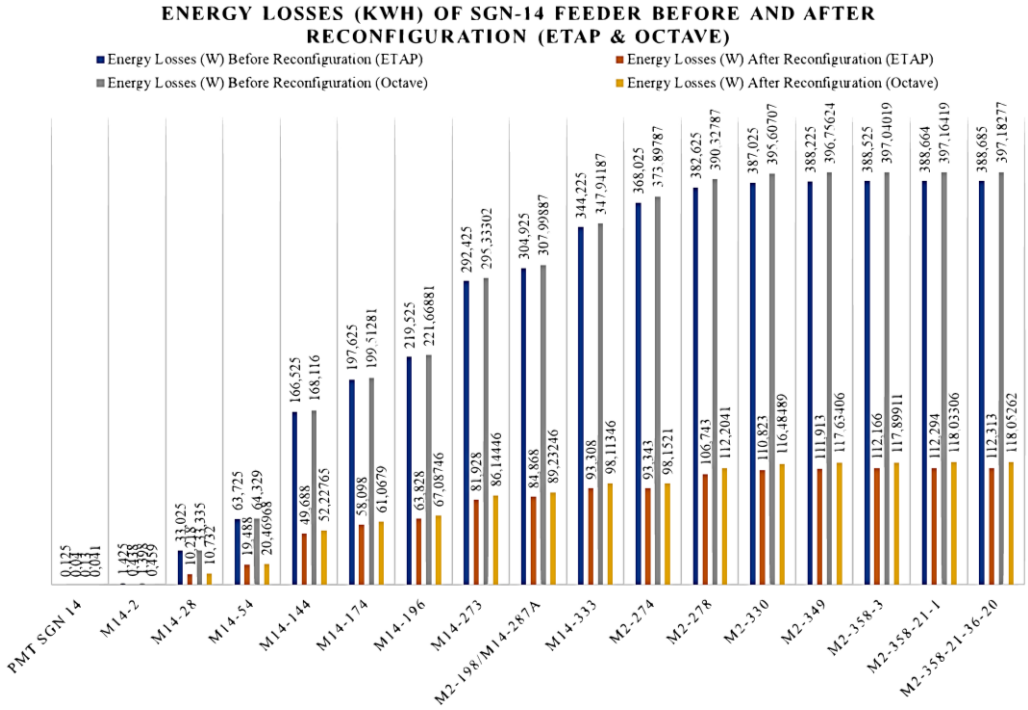

Figure 8. Graph energy losses SGN 14 feeders before and after reconfiguration

3.4.2 SGN 15 Feeder

Figure 9 shows the voltage profile along the newly introduced Feeder SGN-15 after reconfiguration. plotted as percent voltage versus distance from the substation. The SGN-15 feeder was designed to pick up a portion of the load from SGN-14. and its routing near the load centers results in a much gentler voltage drop along its ~20.7 km length. As illustrated. the voltage at the SGN-15 sending end starts at essentially 100% (20 kV base) and declines to around 95% at the far end. The maximum voltage drop on SGN-15 is about 4.9%. which is well within the ±10% limit of SPLN T6.001:2013 and thus meets the required voltage quality standard. The profile is fairly linear and gradual – there are no abrupt large drops as seen previously on SGN-14 – because the feeder's load is distributed and the conductor sizing (a mix of MVTIC and AAAC) is adequate to keep impedance low. In Fig. 9.. the ETAP simulation results (blue curve) and the GNU Octave calculated points (orange curve) for SGN-15 are virtually overlapping. This indicates excellent agreement between the two methods. with only minimal deviations (on the order of a few tenths of a percent) at certain distances. Such close correspondence validates that the SGN-15 feeder model has been correctly implemented and that the analytical calculations echo the simulation. Overall. the SGN-15 voltage profile confirms that the new feeder operates with healthy voltage levels throughout. complementing SGN-14's improved profile so that both feeders remain in compliance with the standard and provide better service voltage to all load points.

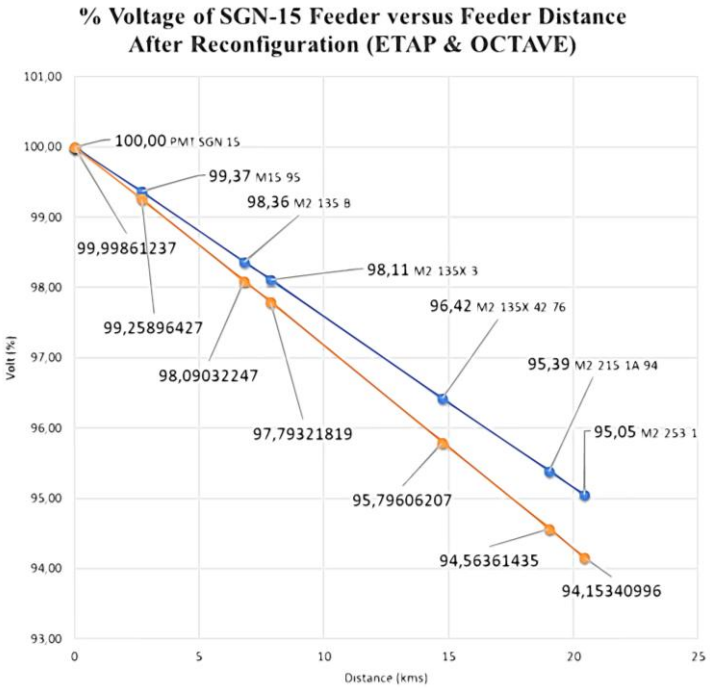

Figure 9. Graph drop voltage SGN 15 feeders before and after reconfiguration

The distribution of power losses along Feeder SGN-15 (after reconfiguration) is depicted in Figure 10. Each pair of bars represents the line loss in watts for a given segment of SGN-15. comparing the ETAP result (blue) with the Octave calculation (orange). Since SGN-15 is a new feeder serving what were previously the distant loads of SGN-14. its losses reflect the fresh load flow path: losses are modest near the substation source and increase somewhat toward the middle/end of the feeder as the cumulative current grows with distance. The largest power loss on SGN-15 occurs at the far end segment. on the order of 81 kW (ETAP estimate) in the final span. Most other sections have lower losses; for example. intermediate segments show tens of kW lost. and the initial sections near "PMT SGN 15" only incur a few kilowatts or less (owing to short distance and the fact that current starts smaller at the source). The total power loss on SGN-15 according to ETAP is about 81.13 kW. which is consistent with the portion of load it carries. The Octave manual calculation yields a very similar total (around 85 kW across the feeder. as seen in the summation at the end node). indicating only a minor discrepancy of a few kilowatts. This corresponds to a small error percentage. demonstrating that the analytical formula-based computation closely matches the software simulation. The alignment of blue and orange bars in Fig. 10. for every segment underscores that the ETAP and Octave analyses are in strong agreement for SGN-15 as well. In summary. SGN-15's post-reconfiguration losses are moderate and expected for the feeder's length and load – and crucially. the addition of this feeder has relieved SGN-14 such that the combined system losses (SGN-14 + SGN-15) are much lower than originally on SGN-14 alone.

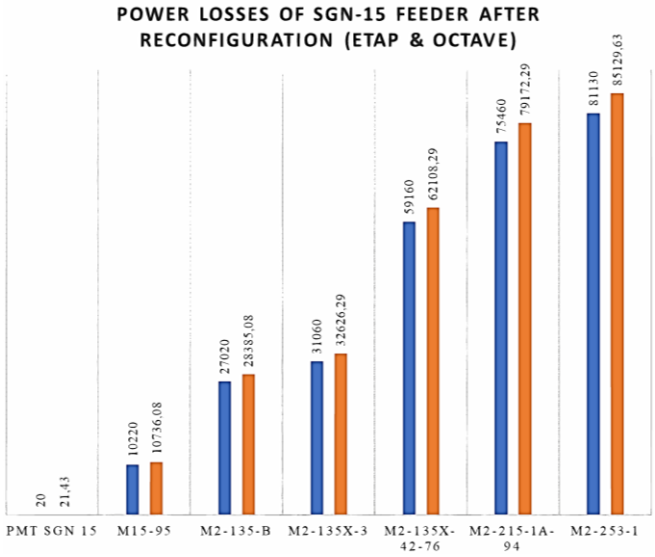

Figure 10. Graph power losses SGN 15 before and after reconfiguration

Figure 11 provides a comparison of energy losses (in kWh) per section along SGN-15 after reconfiguration. paralleling the power loss analysis. As anticipated. the energy loss profile follows the same trend as the instantaneous power losses – sections with higher watt losses correspond to higher kWh losses over the period considered. The results from ETAP (blue bars) and Octave (orange bars) for energy lost are nearly indistinguishable. indicating that over the simulated timeframe the two methods concur on how much energy each line segment dissipates. The largest energy loss occurs at the end of the feeder. roughly 81.13 kWh at the final segment according to ETAP. versus 85.13 kWh by Octave's calculation (assuming a one-hour reference period). This slight difference (on the order of 4 kWh. or ~5%) is consistent with the small power loss discrepancy noted earlier. and it reinforces the high accuracy of the ETAP model in predicting energy dissipation. Overall. SGN-15 experiences about 81 kWh of energy loss during the peak load period (compared to ~388 kWh that SGN-14 was losing before reconfiguration). This confirms that the introduction of SGN-15 has not only split the load but also drastically cut the energy wasted in the system. The one-to-one correspondence between the reduction in power loss and the reduction in energy loss (since energy is power over time) demonstrates internal consistency in the analysis. Moreover. the close match between ETAP and GNU Octave outcomes for both power and energy metrics serves as a mutual validation of the simulation and manual calculation approaches. In summary. the SGN-15 feeder operates with efficient performance. and together with the improved SGN-14. the network's energy losses are far lower than the original configuration. supporting the feasibility and effectiveness of the reconfiguration strategy.

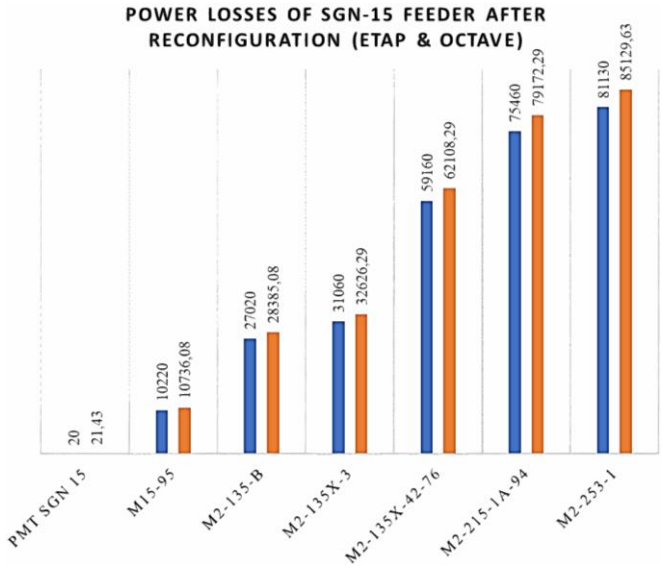

Figure 11. Graph energy losses SGN 15 feeders before and after reconfiguration

As depicted in the single-line diagrams before and after reconfiguration in Figure 12 and 13. the voltage profile of the feeders improves markedly once SGN-15 is introduced. In the pre-reconfiguration SLD (SGN-14 alone). several busbars are highlighted in red. indicating local voltage drops exceeding 10% of nominal voltage – a clear violation of the SPLN T6.001:2013 standard limit. By contrast. after reconfiguration no busbar is colored red. signifying that all voltage drops have been reduced below the 10% threshold. The post-reconfiguration diagram shows bus voltages largely in pink (denoting drops in the 5–10% range) or blue (drops below 5%). reflecting a substantially improved voltage profile across the network. This visual evidence underscores that the network reconfiguration successfully restored compliance with voltage-drop standards and achieved better load distribution. By transferring a portion of SGN-14's load to the new SGN-15 feeder. the system alleviated the overload on SGN-14 and balanced the demand more evenly. thereby improving overall voltage stability and reducing the risk of localized undervoltage conditions.

After the network is reconfigured and part of the load is transferred to feeder SGN-15. all SGN-14 buses rise above 93% so no node is classified as critical and no red buses appear on the ETAP SLD; only the far-end buses M2-278. M2-329. M2-349. M2-358-3. M2-358-21-1. M2-358-21-36-20. and M2-361 remain in the near-critical category with voltages about 93–94%. whereas all upstream buses from PMT SGN-14 through M2-274 are now above 95% and plotted in the normal color. On feeder SGN-15. every bus operates with a voltage of at least 95% of nominal. so there are no critical (red) or near-critical (pink) buses at all. indicating that the new feeder fully satisfies the specified voltage-drop limits.

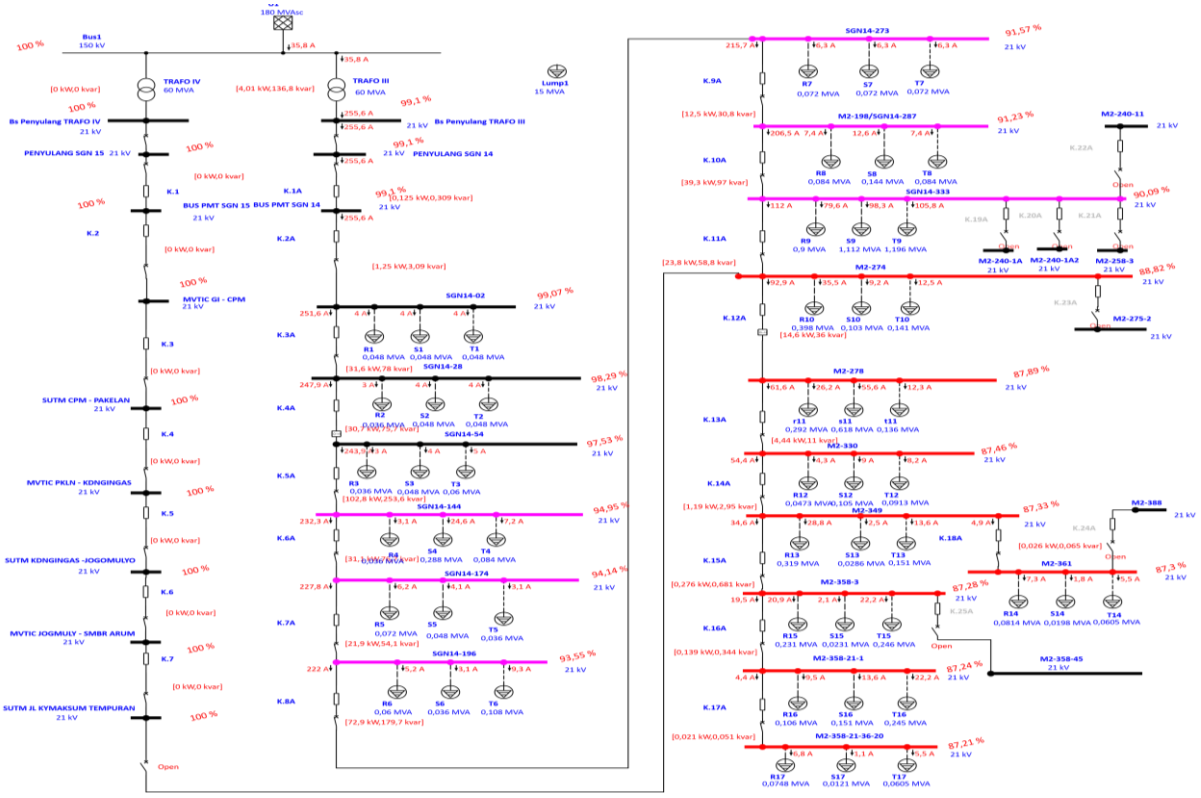

Figure 12. Single line diagram ETAP SGN 14 and 15 Feeder before reconfiguration

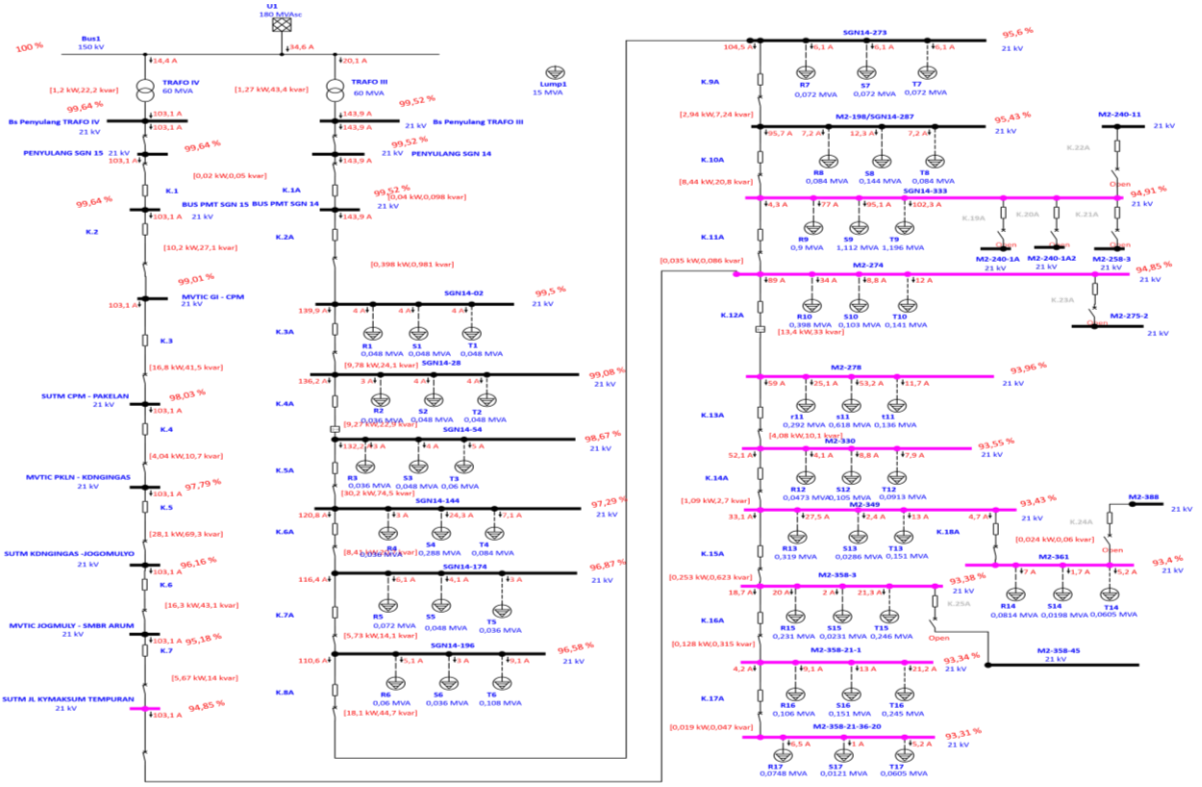

Figure 13. Single line diagram ETAP SGN 14 and 15 Feeder after reconfiguration

Before reconfiguration. SGN-14's far-end bus voltages were as low as about 87% of nominal (exceeding the 10% voltage-drop limit) due to heavy loading. whereas after introducing SGN-15 and transferring part of the load. all SGN-14 buses rose above 93% and all SGN-15 buses exceeded 95%. so that the worst voltage drop decreased from roughly 12.8% to 6.5% on SGN-14 and to only around 4.95% on SGN-15. This behavior is consistent with the general expectation that network reconfiguration or feeder addition improves the voltage profile. and agrees with findings by Alemayehu et al. [9]. who reported an increase in minimum bus voltage from

0.7537 pu to 0.9550 pu. and by Gallego Pareja et al. [5]. who showed that feeder reconfiguration with voltage regulators raises system voltages. In parallel. ETAP results indicate that SGN-14's active losses dropped from 388.711 kW to 112.337 kW (≈71%). while SGN-15 contributes 81.130 kW. yielding a combined loss of about 195.467 kW—roughly half of the original SGN-14 loss and closely matching GNU Octave calculations (difference ≈1–2%). This reduction is comparable to the 72% loss cut reported in the Wolaita Sodo case using DNR plus DG [9]. even though the present study does not employ DG. and lies within the 60–70% range typically achieved by combining DNR with DG or regulator placement [5][6]. Consequently. total energy loss is nearly halved and the loss-related cost decreases from approximately Rp460.32 million/month to Rp231.44 million/month. yielding savings of about Rp228.82 million/month. in line with other reports linking substantial loss reduction to multi-million currency benefits [6][10].

4. CONCLUSION

In conclusion. the proposed SGN-15 feeder effectively alleviated the overload on the existing SGN-14 feeder and enhanced the system's voltage profile. The 20.7 km feeder employs 8.152 m of MVTIC and 12.584 m of AAAC conductors. 238 concrete poles. 836-line accessories. and the requisite switching devices to redistribute part of SGN-14's load. Post-reconfiguration analysis shows that the voltage drops on SGN-14 falls from 12.82% to 6.5%. while SGN-15 operates at about 4.95%. ensuring both feeders comply with the SPLN T6.001:2013 standard (within the 10% voltage-drop limit). Power and energy losses also decrease significantly as a result. On SGN-14. losses drop from 388.711 W (388.711 kWh) to 112.337 W (112.337 kWh). while SGN-15 contributes 81.130 W (81.130 kWh). yielding total losses of 195.467 W (195.467 kWh) after reconfiguration. This reduction produces substantial cost savings: monthly loss costs fall from Rp460.32 million to Rp231.44 million. saving about Rp228.82 million per month. These outcomes align with related literature on feeder load-splitting. confirming that SGN-15 is both technically feasible and economically justified for PLN ULP Magelang. Overall. the implementation of SGN-15 is supported as a prudent long-term investment to improve the network's performance.

REFERENCE

[1] F. O. Akpojedje and E. A. Ogujor. "Optimal network reconfiguration of electric power distribution system for power loss reduction and voltage profile improvement." *Journal of Energy Technology and Environment*. vol. 3. no. 1. 2021. https://doi.org/10.37933/nipes.e/3.1.2021.6

[2] T. Jayabarathi. T. Raghunathan. N. Mithulananthan. S. H. C. Cherukuri. and G. L. Sai. "Enhancement of distribution system performance with reconfiguration. distributed generation and capacitor bank deployment." *Heliyon*. vol. 10. no. 7. Art. no. e26343. 2024. https://doi.org/10.1016/j.heliyon.2024.e26343

[3] N. Gholizadeh and P. Musilek. "A generalized deep reinforcement learning model for distribution network reconfiguration with power flow-based action-space sampling." *Energies*. vol. 17. no. 20. Art. no. 5187. 2024. https://doi.org/10.3390/en17205187

[4] Z. Hu. H. Zhu. and C. Deng. "Distribution network reconfiguration optimization method based on undirected-graph isolation group detection and the whale optimization algorithm." *AIMS Energy*. vol. 12. no. 2. pp. 484–504. 2024. https://doi.org/10.3934/energy.2024023

[5] L. A. Gallego Pareja. J. M. López-Lezama. and O. Gómez Carmona. "Optimal feeder reconfiguration and placement of voltage regulators in electrical distribution networks using a linear mathematical model." *Sustainability*. vol. 15. no. 1. Art. no. 854. 2023. https://doi.org/10.3390/su15010854

[6] B. Alemayehu. S. Mishra. G. G. Tejani. and S. Tripathi. "Network reconfiguration and DG based compensation of Wolaita Sodo distribution system by using particle swarm optimisation." *PLOS One*. vol. 20. no. 10. Art. no. e0335512. 2025. https://doi.org/10.1371/journal.pone.0335512

[7] J. Tian *et al*.. "Distributed optimization and scheduling strategy for source-load-storage distribution grid based on alliance chain." *AIMS Energy*. vol. 12. no. 5. pp. 946–967. 2024. https://doi.org/10.3934/energy.2024044

[8] A. Gill. P. Singh. J. H. Jobanputra. and M. L. Kolhe. "Placement analysis of combined renewable and conventional distributed energy resources within a radial distribution network." *AIMS Energy*. vol. 10. no. 6. pp. 1216–1229. 2022. https://doi.org/10.3934/energy.2022057

[9] Z. Zhang. W. Du. Y. Lu. G. Xu. and Y. Zhao. "Two-stage robust distribution network reconfiguration against failures of lines and renewable generations." *IEEE Access*. vol. 10. pp. 108614–108624. 2022. https://doi.org/10.1109/ACCESS.2022.3213803

[10] J. Lei *et al*.. "Economic dispatch of distribution network with dispersed wind power considering network reconfiguration." *Frontiers in Energy Research*. vol. 10. Art. no. 942350. 2022. https://doi.org/10.3389/fenrg.2022.942350

[11] S. Malekshah. A. Rasouli. Y. Malekshah. A. Ramezani. and A. Malekshah. "Reliability driven distribution power network dynamic reconfiguration in presence of distributed generation by the deep

reinforcement learning method." *Alexandria Engineering Journal*. vol. 61. no. 8. pp. 6541–6556. 2022. https://doi.org/10.1016/j.aej.2021.12.012

[12] Y. Xu. M. Zhao. H. Wu. S. Xiang. and Y. Yuan. "Coordination of network reconfiguration and mobile energy storage system fleets to facilitate active distribution network restoration under forecast uncertainty." *Frontiers in Energy Research*. vol. 10. Art. no. 1024282. 2023. https://doi.org/10.3389/fenrg.2022.1024282

[13] J. Muñoz. L. Tipán. C. Cuji. and M. Jaramillo. "Resilient distribution system reconfiguration based on genetic algorithms considering load margin and contingencies." *Energies*. vol. 18. no. 11. Art. no. 2889. 2025. https://doi.org/10.3390/en18112889

[14] H. Lotfi. M. E. Hajiabadi. and H. Parsadust. "Power distribution network reconfiguration techniques: A thorough review." *Sustainability*. vol. 16. no. 23. Art. no. 10307. 2024. https://doi.org/10.3390/su162310307

[15] Q. Liu. L. Zhang. X. Ji. and H. Shi. "Dynamic reconfiguration of distribution network considering the uncertainty of distributed generation and loads." *Frontiers in Energy Research*. vol. 11. Art. no. 1279579. 2023. https://doi.org/10.3389/fenrg.2023.1279579

[16] O. M. Neda *et al*.. "Distribution system reconfiguration for enhancing techno-economic advantages using a novel technique: A case study of Al-Fuhood substation. Iraq." *Progress in Engineering Science*. vol. 2. no. 3. Art. no. 100124. 2025. https://doi.org/10.1016/j.pes.2025.100124

[17] F. Bohigas-Daranas. O. Gomis-Bellmunt. and E. Prieto-Araujo. "Open-source implementation of distribution network reconfiguration methods: Analysis and comparison." *arXiv preprint arXiv:2511.22957*. 2025. Available: https://arxiv.org/abs/2511.22957

[18] A. Owosuhi. Y. Hamam. and J. Munda. "A new framework for active loss reduction and voltage profile enhancement in a distributed generation-dominated radial distribution network." *Applied Sciences*. vol. 14. no. 3. Art. no. 1077. 2024. https://doi.org/10.3390/app14031077

[19] Z. Pei. J. Chen. Z. Zhang. W. Liu. X. Yan. and Y. Jin. "Opinions on dynamic topology reconfiguration of distribution networks for PV hosting capacity enhancement." *Frontiers in Energy Research*. vol. 12. Art. no. 1512790. 2024. https://doi.org/10.3389/fenrg.2024.1512790

[20] X. Li. M. Li. M. Yu. and Q. Fan. "Fault reconfiguration in distribution networks based on improved discrete multimodal multi-objective particle swarm optimization algorithm." *Biomimetics*. vol. 8. no. 5. Art. no. 431. 2023. https://doi.org/10.3390/biomimetics8050431

[21] Y. Yu. M. Yang. Y. Zhang. P. Ye. X. Ji. and J. Li. "Fast reconfiguration method of low carbon distribution network based on convolutional neural network." *Frontiers in Energy Research*. vol. 11. Art. no. 1102949. 2023. https://doi.org/10.3389/fenrg.2023.1102949